Environmental Pollution 260 (2020) 114027

Contents lists available at ScienceDirect

Environmental Pollution

journal homepage: www.elsevier.com/locate/envpol

Relative contributions of a major international airport activities and other urban sources to the particle number concentrations (PNCs) at a nearby monitoring site☆

Milad Pirhadi [a], Amirhosein Mousavi [a], Mohammad H. Sowlat [a], Nicole A.H. Janssen [b], Flemming R. Cassee [b, c], Constantinos Sioutas [a, *]

[a] University of Southern California, Department of Civil and Environmental Engineering, Los Angeles, CA, USA
[b] National Institute for Public Health and the Environment (RIVM), Bilthoven, Netherlands
[c] Institute for Risk Assessment Studies, Utrecht University, Utrecht, Netherlands

ARTICLE INFO

Article history:
Received 9 August 2019
Received in revised form
25 December 2019
Accepted 19 January 2020
Available online 25 January 2020

Keywords:
Airport emissions
Aviation
Source apportionment
Positive matrix factorization (PMF)
Traffic emissions

ABSTRACT

In this study, the positive matrix factorization (PMF) source apportionment model was employed to quantify the contributions of airport activities to particle number concentrations (PNCs) at Amsterdam Schiphol. Time-resolved particle number size distributions in parallel with the concentrations of auxiliary variables, including gaseous pollutants (NO_x and CO), black carbon, $PM_{2.5}$ mass, and number of arrivals/departures were measured for 32 sampling days over a 6-month period near Schiphol airport to be used in the model. PMF results revealed that airport activities, cumulatively, accounted for around 79.3% of PNCs and our model segregated them into three major groups: (i) aircraft departures, (ii) aircraft arrivals, and (iii) ground service equipment (GSE) (with some contributions of local road traffic, mostly from airport parking lots). Aircraft departures and aircraft arrivals showed mode diameters <20 nm and contributed, respectively, to 46.1% and 26.7% of PNCs. The factor GSE/local road traffic, with a mode diameter of around 60–80 nm, accounted for 6.5% of the PNCs. Road traffic related mainly to the surrounding freeways was characterized with a mode diameter of 30–40 nm; this factor contributed to 18.0% of PNCs although its absolute PNCs was comparable with that of areas heavily impacted by traffic emissions. Lastly, urban background with a mode diameter at 150–225 nm, had a minimal contribution (2.7%) to PNCs while dominating the particle volume/mass concentrations with a contribution of 58.2%. These findings illustrate the dominant role of the airport activities in ambient PNCs in the surrounding areas. More importantly, the quantification of the contributions of different airport activities to PNCs is a useful tool to better control and limit the increased PNCs near the airports that could adversely impact the health of the adjacent urban communities.

1. Introduction

Ultrafine particles (UFPs) have the potential to cause adverse health impacts due to their chemical composition, oxidative capacity, high surface area to particle mass ratio, and their ability to reach the lung alveoli (Chen et al., 2016; Cheng et al., 2016; Delfino et al., 2005). Although UFPs comprise typically a minor part of the ambient PM mass, they contribute to the majority of ambient particle number concentrations (PNCs) (Harrison et al., 2011; Keywood et al., 1999; Ruuskanen et al., 2001; Stanier et al., 2004).

Several studies have documented airports as major sources of UFPs (Hsu et al., 2014; Hu et al., 2009; Hudda and Fruin, 2016; Mazaheri et al., 2013; Shirmohammadi et al., 2017; Westerdahl et al., 2008). However, there are still uncertainties associated with the impact of specific airport activities on the PNC increase in the adjacent communities based on studies conducted in different locations near major airports around the globe (Hsu et al., 2014; Hudda et al., 2014; Masiol et al., 2017). For example, while Masiol et al. (2017) reported that the impacts of the London Heathrow (LHR) airport activities on PNC in an urban location near the airport is around two thirds of those of the road traffic activities, the

☆ This paper has been recommended for acceptance by Admir Créso Targino.

* Corresponding author. 3620 S. Vermont Ave. KAP210, Los Angeles, CA, 90089, USA.
E-mail address: sioutas@usc.edu (C. Sioutas).

https://doi.org/10.1016/j.envpol.2020.114027
0269-7491/

impacts of the Los Angeles International Airport (LAX) emissions on the PNC in the populated areas downwind of the airport are substantially higher than those of the adjacent freeways (Hudda et al., 2014; Shirmohammadi et al., 2017). According to the International Civil Aviation Organization (ICAO), landing and takeoff (LTO) cycle consists of the following operational modes: landing (approach), taxing/idling, takeoff, and climb-out (Mazaheri et al., 2011). Landing is considered as the arrival phase, and takeoff that is immediately followed by climb-out are considered as the departure phase. It should be noted that each arrival and departure activity includes taxing/idling as well. Furthermore, airport ground service equipment (GSE) emissions, which include different ground-based activities such as diesel-engine passenger buses, heavy duty vehicles (HDVs) to transport luggage, fuel and supply, ground power units, and tugs (Targino et al., 2017), may contribute significantly to the overall air pollution produced by airports. Non-combustion sources (e.g., road dust, tire and brake wear, and soil) are dominated by larger particles (i.e., $\geq$1 μm) with negligible contributions to PNCs (Gietl et al., 2010; Harrison et al., 2012). A few previous studies were mostly focused on the takeoff and landing processes as major parts of the aircraft departure and arrival phases, respectively (Hu et al., 2009; Mazaheri et al., 2008; Ren et al., 2016; Westerdahl et al., 2008). Moreover, some studies such as the Aircraft Particle Emissions eXperiment (APEX) campaigns investigated emissions from multiple commercial aircraft engine models (Beyersdorf et al., 2014; Kinsey, 2009; Kinsey et al., 2010; Onasch et al., 2009; Wey et al., 2007, 2006). Based on the findings of these studies, PNC increases due to aircraft activities might vary within orders of magnitude depending on parameters such as the distance from the jet engine exhaust, engine type, fuel type, wind direction/frequency, and ambient conditions (e.g., temperature and relative humidity) even in a single runway of the airport. Therefore, it would be essential to quantify the ultimate impact (contribution) of these activities on daily PNCs measured in the urban areas affected by airport emissions.

Previous positive matrix factorization (PMF) source apportionment models were able to resolve only one factor attributed to airport emissions (Masiol et al., 2017, 2016). The quantitative contribution of specific major airport activities (e.g., aircraft departures, aircraft arrivals, and GSE) to the PNCs in the nearby urban areas is essential in order to fully understand the sources of increased PNCs in these areas. In this study, we quantified the contribution of major airport activities as well as other pollution sources to the PNCs in an urban area near Amsterdam Schiphol airport, the 3rd busiest airport in Europe. A strong association between PNCs downwind of Schiphol airport and flight activity has been observed in an earlier study (Keuken et al., 2015) which further underpins the need for conducting detailed source apportionment of the observed PNC, which will enable the promulgation of effective emission mitigation strategies to reduce population exposure to these air pollutants.

2. Methodology

2.1. Sampling site

Fig. 1 illustrates the location of the sampling site (52° 19′ 15.2″ N, 4° 47′ 7.5″ E) which was located approximately 2 km from northeast of the airport and 300 m from two major runways. Four runways of the airport, including 09/27, 18L/36R, 06/24, and 18C/36C, are located to the southwest of the sampling site, whereas the runway 18R/36L is located to the northwest of the sampling site at a distance of 5.7 km. It is noteworthy that the runway 04/22 is typically used for small aircraft; thus, we were not expecting to

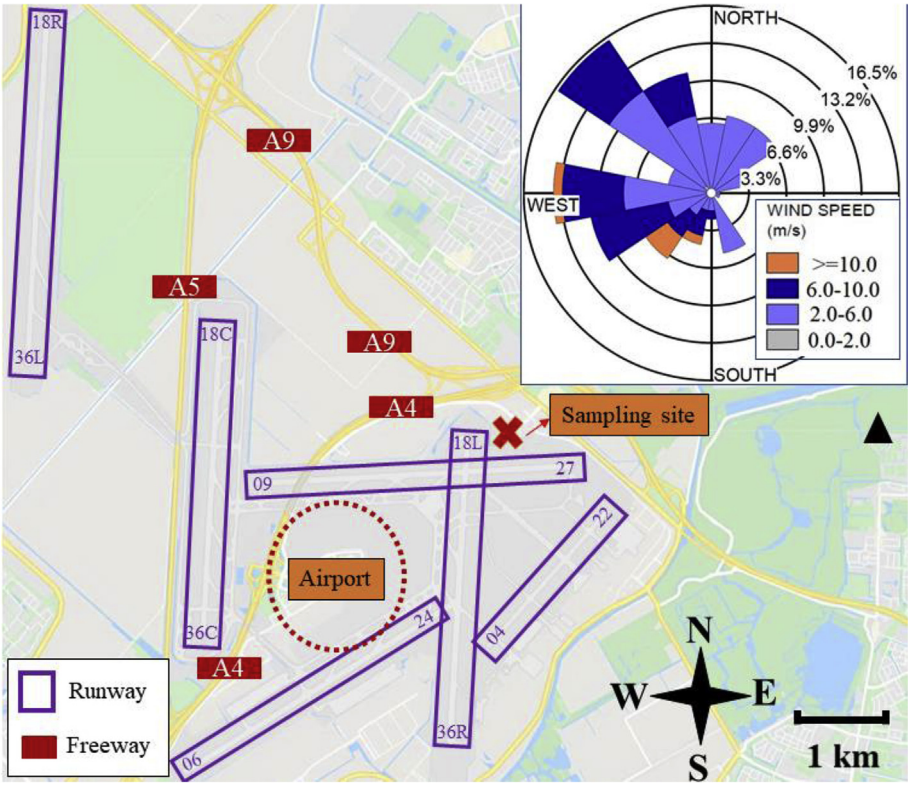

Fig. 1. (a) Location of the sampling site with respect to the Schiphol airport, main runways, and major freeways. The wind rose during the study period is also shown in the top-right corner of the figure. Moreover, the black triangle shown in the right side of the figure indicates the sampling site of the Keuken et al. (2015) study in the same area.

capture significant emissions from this runway. The wind rose during the sampling period is also shown in the right corner of the figure. According to the figure, the dominant wind direction is almost southwesterly, which directly transports airport-related emissions to the densely populated areas to the northeast of the airport. The sampling site is also close by (500–1000 m) two of the local major freeways (i.e., A4 and A9) as well as several large parking lots, and is influenced by the passenger traffic to and from the airport. It should be noted that based on the local wind patterns, a major part of these freeways are located upwind of the sampling site. Thus, our sampling site represents an environment that is impacted by both the emissions from nearby airport activities as well as road traffic.

2.2. Sampling period and instrumentation

Measurements, in the framework of a human volunteer exposure study investigating health impacts of air pollution, were conducted inside a mobile exposure laboratory from May through October 2018 with a total of 32 sampling days. In the exposure chamber (volume of 14 m^3), an airflow system was present to keep the air displacement level constant and to obtain a uniform flow of ambient air (approximately 400 m^3/h). Each day, measurements were carried out approximately from 10 a.m. or earlier to around 3 p.m. The meteorological parameters during the sampling campaign were obtained from the Royal Netherlands Meteorological Institute (KNMI). The average temperature, wind speed, and relative humidity during the sampling campaign were 19.9 ± 4.3 °C, 5.1 ± 2.2 m/s, and 63.5 ± 11.6%, respectively. Although we limited the sampling period to 5 h per day, we do not expect our main findings regarding the model-resolved contributions of airport and traffic activities to PNCs to change considerably, based on the evidence provided by Keuken et al. (2015). The authors of that study observed that the net average PNCs (i.e., concentrations when the wind direction was from Schiphol airport subtracted by the background concentrations) based on high-resolution data measured downwind of the airport between 10 a.m. and 3 p.m. differed less than 5% from the daily average. Moreover, more than 95% of the air traffic activity at Schiphol airport and 90% of the road traffic activity of the adjacent freeways (i.e., A4 and A9) take place during the 6 a.m. to 11 p.m. period, making the nighttime data of little relevance.

The measurement campaign aimed to capture days with predominant winds blowing from the airport and nearby runways, or winds coming from the opposite site which would result in mostly road traffic and other urban emissions, and was not designed to capture the local seasonal patterns. However, based on the flight activity (Fig. S3), traffic counts on the adjacent freeways (Fig. S4), wind direction patterns (Table S4), and other meteorological conditions such as mixing height (section 1 of SI), this period captures the annual patterns of some of these parameters affecting PNCs. As shown in Figs. S3 and S4, the variations in flight activity and road traffic counts from month-to-month are very low (the ratio of standard deviation to average was less than 8%); therefore, our sampling period captures adequately the yearly patterns of air traffic at the airport as well as the road traffic in the surrounding freeways. We also calculated the annual local wind frequency using the high-resolution data (resolution of 30 min) over the year 2018 provided by the Weather Underground (The Weather Company, GA, US) as shown in Table S4. It was observed that the wind blew from the Schiphol airport location to our sampling site (i.e., SSW, SW, and WSW directions in Table S4) around 18% of the time over the year 2018, while that fraction during our 6-month sampling period was around 17%. Thus, our sampling period reflects closely the annual wind patterns of the region. More discussion about the limitations of the collected dataset is provided in section 3.1.

Ambient particle number size distributions in the range of 10–225 nm were measured utilizing a scanning mobility particle sizer (SMPS, Model 3936, TSI Inc., Shoreview, MN, USA) connected to a nano water-based condensation particle counter (CPC, Model 3788, TSI Inc., Shoreview, MN, USA). A sample flow of 1.5 L/min and a sheath flow of 15 L/min were used for the SMPS measurements. The size distribution of particles in the range of 10–225 nm was measured in 88 size channels with a time resolution of 2 min. Prior to conducting the field experiments, the SMPS and CPC instruments were sent to the manufacturing company (i.e., TSI Inc.) for calibration. Additionally, a tapered element oscillating microbalance (TEOM, Model 1405, Thermo Fisher Scientific Inc., Waltham, MA, USA) was utilized to continuously monitor the ambient $PM_{2.5}$ mass concentrations. The flow rate of the TEOM instrument was 5 L/min. Black carbon (BC) concentrations were monitored with a time resolution of 1 min by employing a portable Aethalometer (MicroAeth Model AE51, Magee Scientific, Berkeley, CA, USA). The model AE51 operating with radiation source of 880 nm utilizes a T60 Teflon-coated borosilicate glass fiber filter strip for particle collection and subsequent BC analysis. The AE51 flow rate was 0.1 L/min. In order to calculate the instrument's limit of detection (LoD), we used the approach followed by Targino et al. (2017). A HEPA filter (Model No. 12144, Pall Laboratory, Ann Arbor, MI, USA) was fitted to the AE51 inlet and the instrument was run for 13 h. The instrument's LoD calculated as (LoD = 3*standard deviation of the data under the abovementioned operating condition) was approximately 0.095 μg BC/m^3. In addition, measurements of gaseous pollutants such as nitrogen oxides and carbon monoxide (NO_x and CO) were conducted using continuous monitors. NO_x concentrations were monitored using a chemiluminescent NO-NO_2-NO_x analyzer (Model 200E, Advanced Pollution Instrumentation (T-API), San Diego, CA, USA). The sample flow rate of the instrument was 0.5 L/min. Moreover, the span noise was 0.2 ppb while the zero noise was <0.2 ppb. A gas filter correlation analyzer (Model 300E/EM, T-API, San Diego, CA, USA) was employed to monitor the CO concentrations. Sample flow rate of this instrument was 0.8 L/min. The span noise and zero noise were, respectively, 0.02 ppm and <0.02 ppm. It should be noted that the data of NO_x and CO concentrations were recorded with a resolution of 10 s using a Squirrel SQ 2020 data logger (Grant Instruments Ltd., Cambridge, UK).

2.3. PMF model

PMF is a widely-used receptor model which can be utilized to identify the sources of and quantify their contributions to a specific variable (in this study, total ambient PNC) (Hopke, 2016; Paatero et al., 2014). This receptor model employs a multivariate technique to solve the following mathematical equation (Krecl et al., 2008):

$$x_{ij} = \sum_{k=1}^{p} g_{ik} f_{kj} + e_{ij} \quad (1)$$

where x_{ij} refers to the ambient PNC (or another auxiliary variable concentration) of the ith sample and jth size interval (or species), p refers to the number of factors which contribute to the ambient PNCs, g_{ik} refers to the relative contribution of factor k to sample i, f_{kj} is the ambient PNC of jth size interval in the kth factor, and e_{ij} represents the residual error value (observed − predicted) of the sample i and size interval j. Subsequently, using a weighted least-squares approach, PMF attempts to find out the factor profiles as well as the contributions by minimizing the objective function (Q), which is defined as below:

$$Q = \sum_{i=1}^{n}\sum_{j=1}^{m}\left(\frac{e_{ij}}{u_{ij}}\right)^2 \quad (2)$$

where, n represents the total number of samples, m is the total number of size intervals, and u_{ij} represents the uncertainty of the concentration measurements for the ith sample and jth size interval. PMF performs the abovementioned minimization by implementing the non-negative constraint for source profile and contribution values (Norris et al., 2014).

One major limitation of such receptor models is that the error estimates of environmental data could be considerably varying although it has been shown that the PMF model is better suited than similar dimension reduction methods such as principal component analysis (PCA) (Paatero and Tapper, 1994). Since the exact uncertainty values were not measured for the samples in this study, we used the method suggested by Zhou et al. (2004) to estimate the uncertainties associated with the experimental measurements:

$$S_{ij} = \sigma_{ij} + C_1 \max\left(|x_{ij}|, |y_{ij}|\right) \quad (3)$$

where, S_{ij} is the associated uncertainty for ith sample and jth size interval, C_1 is a constant typically between 0.1 and 0.5, y_{ij} is the predicted value of x_{ij} calculated by the model, and σ_{ij} is the measurement error for ith sample and jth size interval (or species) calculated as follows:

$$\sigma_{ij} = C_2\left(N_{ij} + \overline{N}_j\right) \quad (4)$$

where, C_2 is a constant typically between 0.01 and 0.05, N_{ij} is the predicted number concentration for the ith sample and jth size interval (or species), and $\overline{N}_j$ is the mean number concentration for the jth size interval (or species). In this study, we utilized the USEPA's PMF model version 5.0 for ambient particle number source apportionment. Particle number size distributions in addition to the auxiliary variables, including gaseous pollutants (NO_x and CO), $PM_{2.5}$ mass, black carbon, and flight activity (i.e., number of departures and arrivals) were used as the input to the model. The time resolution for all of the input parameters was 10 min. PMF runs were performed in the robust mode in order to decrease the impacts of the values with considerable uncertainties on the final PMF results (Brown et al., 2015). PNC was selected to be the total variable. Moreover, NO_x, BC, $PM_{2.5}$, and CO were set as weak to minimize their impact on the final solution. In order to evaluate the validity of the PMF outputs, error estimation methods, including Bootstrap (BS) and Displacement (DISP), were used. For the BS analysis, 20 runs were conducted, and the results were considered as acceptable only if all of the resolved factors showed a mapping of above 80%. For the case of DISP analysis, the final solution was associated with no rotational ambiguity if the reduction in Q value (dQ) was less than 0.1% and no factor swap occurred for the lowest dQ_{max}.

3. Results and discussion

3.1. Overview of the data

Table 1 illustrates a statistical summary of the measured species concentrations during the study period. The signal-to-noise ratios (S/N) for all of the measured parameters are significantly higher than unity. The mean total PNC was 35,308 ± 615 particles/cm^3, which is comparable to the day-time average PNC of 42,000 particles/cm^3 reported by Keuken et al. (2015) in an urban area northeast of Schiphol airport when the wind direction was from the airport location. Average particle number and also volume size distributions during the sampling period are shown in Fig. 2. As demonstrated in the figure, the number mode diameter is in the range of 10–20 nm, which is consistent with the other studies conducted in areas affected by the airports (Mazaheri et al., 2008; Westerdahl et al., 2008; Zhu et al., 2011). Further, the average particle volume size distribution was also following the typical trend in the urban areas, with an increase in the total volume concentration as the particle diameter increases especially at size ranges above 100 nm. As expected, the very large number concentrations of smaller particles (i.e., smaller than 30–40 nm) does not have significant impacts on the volume size distribution (Vu

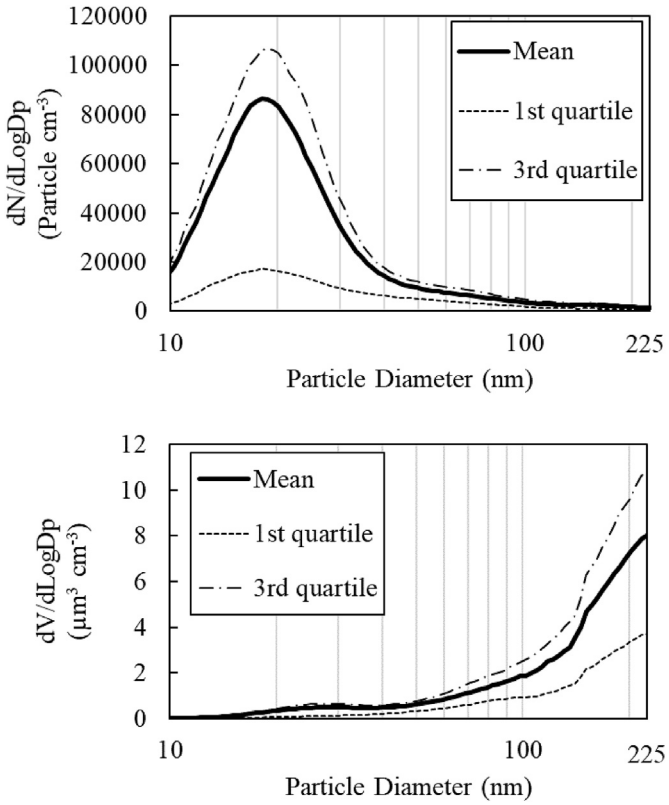

Fig. 2. Average particle number and volume size distributions during the study period. The 1st and 3rd quartiles of the size distributions are also shown in the figures.

Table 1
Statistical summary of the measured concentrations used as input to the PMF model. Resolution of the data is 10 min.

Variable	Mean	Standard error (SE)	Min	Max	S/N ratio
Total number concentration (Particles/cm^3) (SMPS basis)	35,308	615	2080	294,238	7.0
$PM_{2.5}$ (μg/m^3)	7.4	0.3	0.6	99.1	7.1
BC (μg/m^3)	0.6	0.1	0.1	5.3	6.9
NO_x (μg/m^3)	31.8	0.7	4.9	115.6	6.8
CO (μg/m^3)	597.8	3.4	420.8	950.9	6.8

et al., 2015).

Although the data collected during the cooler months of our sampling period might be capturing part of the wintertime PNC patterns, it is possible that if our campaign was extended during the winter months, the absolute PNC values might be higher than the campaign average due to the enhanced condensation and partitioning to the particle phase of semi-volatile organic vapors emitted by the prevailing combustion sources (i.e., aircraft and traffic), a result of lower temperatures as well as depression in atmospheric mixing height (Pirhadi et al., 2019). We acknowledge that the lack of wintertime measurements is a limitation of our study; nonetheless, the PNC sources identified in the sampling area (e.g., aviation, road traffic, airport ground-based operations) are mostly combustion processes, the particle emissions of which are a mixture of non-volatile species such as black carbon (and to a lesser extent trace elements), but mostly semi volatile organic species of similar chemical and thermodynamic properties (He et al., 2018; Kinsey et al., 2011; Mazaheri et al., 2011; Onasch et al., 2009; Shirmohammadi et al., 2018). The PM emissions of these sources would probably be affected to the same degree by the meteorological factors noted earlier. For example, in a study conducted at the Heathrow airport in London, where the meteorological conditions are comparable with those of Amsterdam, Masiol et al. (2017) did not observe considerable differences between the contribution of the apportioned factors to PNCs in warm (i.e., August and September) and cold (i.e., December and January) phases of that study. Specifically, the contribution of the airport factor to PNCs only varied 1.5% between the warm and cold periods. We therefore believe that the relative contributions of the apportioned factors/sources to PNCs in the wintertime would not be substantially different than what is reported in our study, recognizing, again, that this is a limitation and could be the subject of future investigations.

3.2. Number of factors

We performed the PMF runs using various number of factors, uncertainty matrices for the input data, and the PMF extra modeling uncertainty to empirically achieve the most efficient and plausible results in terms of statistical robustness and physical interpretation. More comprehensive discussion on the extra modeling uncertainty selection and the implemented criteria (e.g., factor specific number and volume size distributions, correlation with auxiliary variables and model coefficient of determination (R^2)) to select the best PMF solution is provided in the SI document. Based on the mentioned criteria, a five-factor solution (identified as aircraft arrivals, aircraft departures, road traffic, ground service equipment (GSE)/local road traffic, and urban background, as justified below in more detail) was selected as the optimum result of the PMF model. The predicted versus measured total PNC for the whole study period can be found in the SI section (Fig. S5). As shown in the figure, the R^2 value for the linear regression is 0.99, indicating that the PMF model successfully identified and quantified the sources of the ambient PNC in the study area. A sensitivity analysis was also performed to select the optimum number of factors identified by the PMF model, the details of which can be found in the SI document.

Fig. 3 illustrates the particle number and volume size distributions for each of the resulting factors. The error bars in Fig. 3 represent the uncertainty estimated from the DISP error estimation analysis. Moreover, the explained variation for each of the size bins with corresponding values at the secondary Y-axis can be observed in the size distribution plots. Table 2 tabulates the relative contribution to total PNCs in addition to the auxiliary variable loadings for each of the resulting factors. The absolute contribution (particles cm^{-3}) of each of the PMF-resolved factors to the total PNC

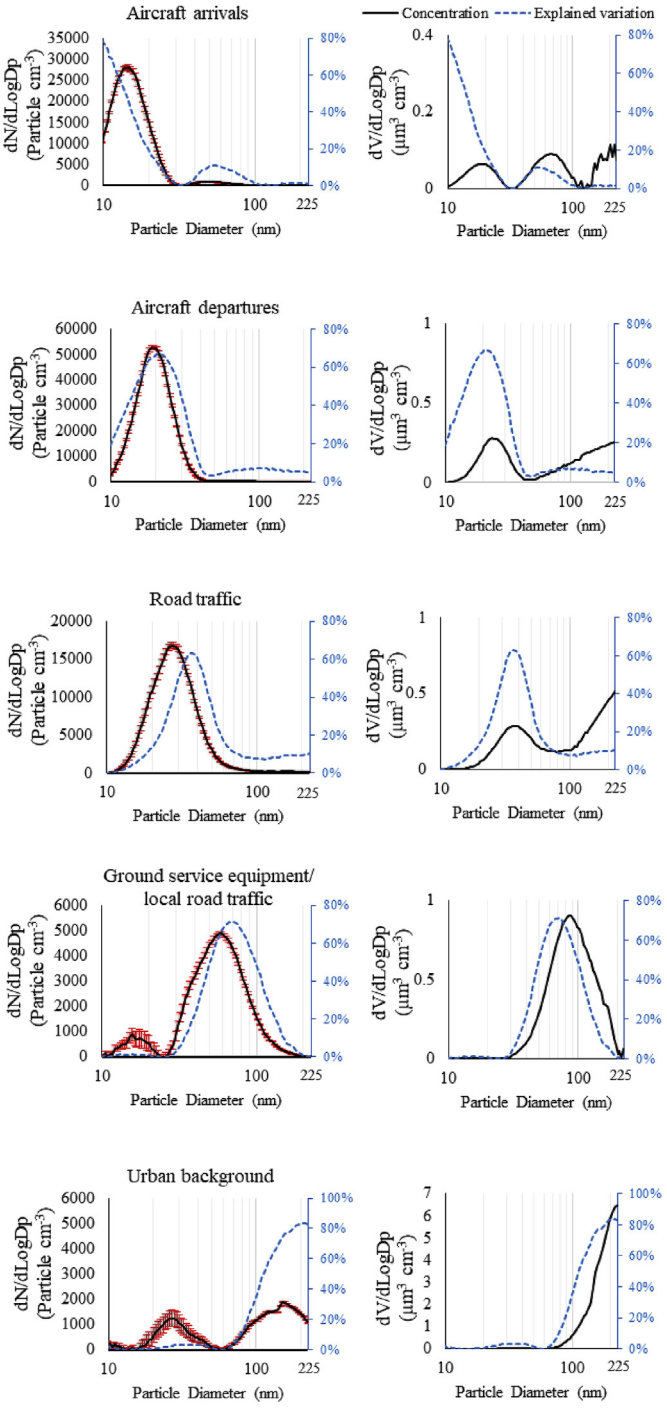

Fig. 3. Number and volume size distributions for each of the resolved factors by the PMF model. The dotted blue lines indicate the explained variation for each of the size bins with corresponding values at the secondary Y-axis, while the solid black lines indicate the absolute concentrations for each of the size intervals with corresponding values at the primary Y-axis. Error bars (in red) represent the uncertainty computed using the displacement (DISP) analysis. (For interpretation of the references to colour in this figure legend, the reader is referred to the Web version of this article.)

is also presented in Fig. 4. PNC pollution roses for each of the resolved factors are also illustrated in Fig. 5.

3.3. Factor identification

Factors 1 and 2 (Aircraft arrivals and Aircraft departures,

Table 2
Relative contribution to total PNCs in addition to the auxiliary variable loadings for each of the resolved factors. In the second column, the values in parenthesis show the range of DISP uncertainty analysis.

Factor name	Mode (nm)	Contribution to PNCs (%)	Auxiliary variable loadings (%)					
			PM mass	NO_x	CO	BC	Departures	Arrivals
Aircraft arrivals	13	26.7 (26.1–27.6)	13	13	24	8	0	45
Aircraft departures	19	46.1 (45.2–46.7)	0	14	0	15	37	0
Road traffic	30–40	18.0 (17.5–18.7)	14	8	12	67	0	0
Ground service equipment (GSE)/local road traffic	60–80	6.5 (6.1–6.9)	13	35	31	10	40	26
Urban background	150–225	2.7 (2.3–3.1)	60	30	33	0	23	29

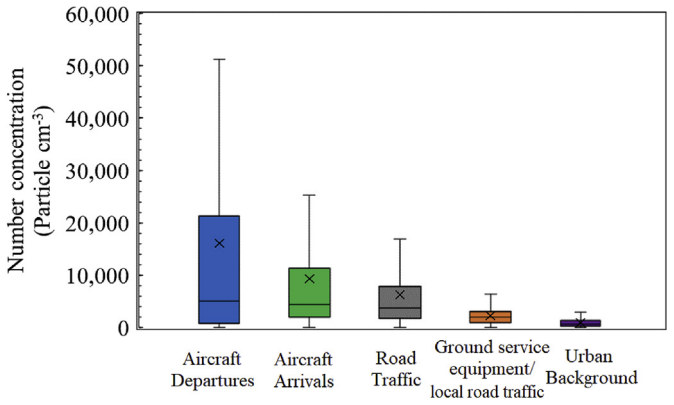

Fig. 4. Absolute contribution (particle cm^{-3}) of each of the PMF-resolved factors to the total particle number concentrations (PNCs).

respectively): Factors 1 and 2 exhibit number modes < 20 nm (i.e., around 13 nm for factor 1 and around 19 nm for factor 2) (Fig. 3) accounting, cumulatively, for the majority of particles < 20 nm (i.e., significantly high explained variations for particles in this size range (secondary Y-axis)). The volume mode diameter for both of these factors is also around 20 nm, although they show another peak in the volume distribution at larger diameters. Factor 1 contributes to 26.7% of PNCs and 2.8% of particle volume concentrations, whereas factor 2 contributions to PNCs and particle volume concentrations are 46.1% and 8.9%, respectively (Table 2). The corresponding absolute contribution of factors 1 and 2 to total PNCs was, respectively, 9357 particles/cm^3 and 16,115 particles/cm^3 (Fig. 4). A previous study conducted in the same area indicated that particle number size distributions in a region affected by the Schiphol airport emissions are dominated by particles in the range of 10–20 nm when the wind was from the airport location (Keuken et al., 2015). Moreover, several studies have documented that aircraft engines emit particles with number mode diameters of <20 nm (Herndon et al., 2008; Kinsey et al., 2010; Lobo et al., 2012; Masiol and Harrison, 2014; Mazaheri et al., 2013). In a similar source apportionment study near the LHR airport using PMF, Masiol et al. (2017) also reported an airport factor with a number mode diameter at around 15 nm.

Factor 1 also demonstrates loadings of NO_x, CO, and BC, all of which are products of aircraft engine emissions (Dodson et al., 2009; Hu et al., 2009; Targino et al., 2017; Vu et al., 2015) (Table 2). Moreover, this factor shows a very strong association (i.e., 45% factor loading) with number of arrivals at the airport while there is no association between this factor and number of departures. On the other hand, factor 2 is correlated with aircraft engine products (e.g., NO_x and BC) and has a high association with number of departures at the airport (37% factor loading), while there is no correlation with the number of arrivals. Therefore, factors 1 and 2 were labelled aircraft arrivals and aircraft departures, respectively. Moreover, as mentioned earlier, the number mode diameter of factor 1 (i.e., aircraft arrivals) is slightly smaller than that of factor 2 (i.e., aircraft departures), which also has been observed by previous studies investigating the PN distribution of aircraft engines (Mazaheri et al., 2008; Westerdahl et al., 2008). This small difference might be attributed to higher thrust settings during aircraft departures (Beyersdorf et al., 2014; Delhaye et al., 2017).

The cumulative contribution of aircraft departures and arrivals to PNCs is 72.8**%.** As mentioned in the introduction section, Keuken et al. (2015) have reported that 77% of the elevated PNC variations downwind of Schiphol airport can be explained by aviation activities. Therefore, the range of contributions to total PNC of aircraft departure and arrival related factors in our study (72.8%) is in agreement with the findings of the previous literature. Moreover, the contribution of aircraft departures to PNCs is around 1.7 times of that of aircraft arrivals. Previous studies have observed a wide range of particle emission trends at different aircraft thrust settings depending on many parameters such as engine type, distance from the jet engine exhaust, and ambient conditions as mentioned earlier (Beyersdorf et al., 2014; Herndon et al., 2008; Hu et al., 2009; Kinsey, 2009; Kinsey et al., 2010; Mazaheri et al., 2011, 2008; Onasch et al., 2009; Ren et al., 2016; Westerdahl et al., 2008; Wey et al., 2007, 2006). Some studies conducted under real world conditions observed higher PNCs from takeoffs in comparison to landings (Mazaheri et al., 2011, 2008; Ren et al., 2016; Westerdahl et al., 2008). For example, Mazaheri et al. (2008) measured PNCs downwind of a runway covering 207 B737 aircrafts at Brisbane airport, Australia. The average PNCs downwind of takeoff activities was around 1.3 times of that of landing activities. On the other hand, Kinsey et al. (2010) observed higher PNCs at lower thrust settings for most of the engines tested during the APEX campaigns. Onasch et al. (2009) reported that particle emissions at thrust setting of 100% (related to takeoff) can be higher or lower than that of 30% (related to landing) depending on the distance of sampling probe from the engine exit plane. In the present study, our sampling site was closer to the busiest runway of Schiphol airport in terms of number of departures (i.e., runway 06/24) than the busiest runway for arrival activities (i.e., 18R/36L). Moreover, the average number of departures during our sampling campaign was slightly higher (i.e., 13%) than that of arrivals (see Table S1). Also, as reported by previous investigations, in general, the taxing time corresponding to the departure activity is around 2–2.5 times that of arrival activity (Mazaheri et al., 2011). Therefore, the higher contributions of aircraft departures to PNCs compared with arrivals observed in our sampling site are supported by field measurement campaign findings (although the literature is not conclusive) when considering the selected sampling location and aircraft activities at Schiphol airport.

The PNCs pollution rose plots corroborated the origin of the resolved aircraft departure and arrival factors (Fig. 5(a)–(b)). As shown in the figure, the highest contributions for both of these factors occur during southwesterly, westerly, and northwesterly

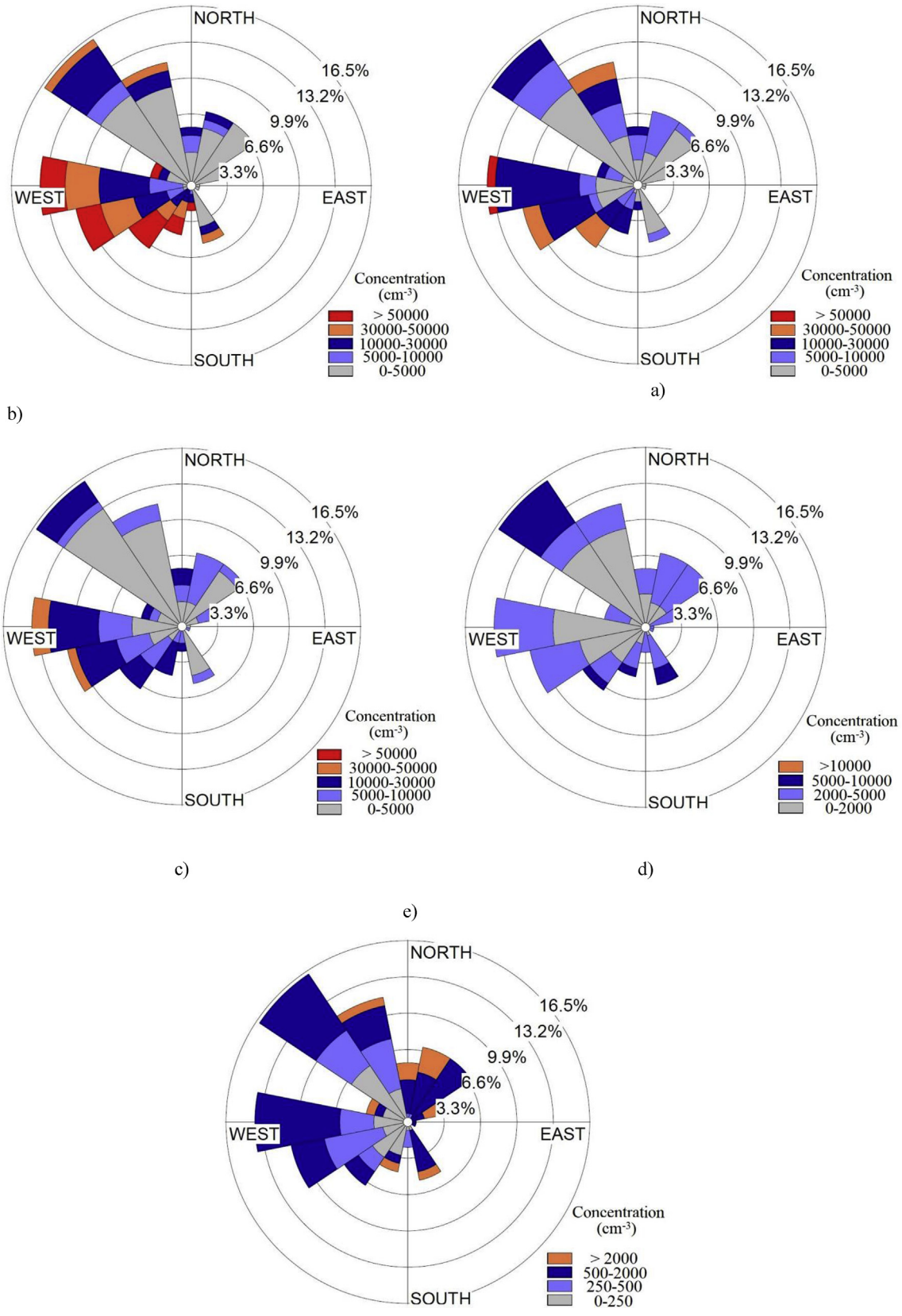

Fig. 5. Particle number concentrations (PNCs) pollution roses for the resolved factors: a) Aircraft departures; b) Aircraft arrivals; c) Road traffic; d) Ground service equipment (GSE)/ local road traffic; e) Urban background.

winds, transporting particles from airport major runways to our sampling site. The contributions from southwest to these factors are higher than those from northwest, mainly because there is only one major runway located to the northwest of the sampling site with a relatively larger distance (i.e., 5.7 km) to the sampling site compared to the other runways, as mentioned in section 2.1.

Factor 3 (Road traffic): Factor 3 is characterized by number (and also volume) mode diameters around 30–40 nm (Fig. 3) and contributes to 18.0% of the total PNCs (Fig. 3 and Table 2). The corresponding absolute contribution of this factor to total PNCs was 6298 particles/cm^3 (Fig. 4). Moreover, the contribution of this factor to total volume/mass concentrations was 12.5%. Particle mode diameters at 30–40 nm have been widely attributed to the road traffic emissions in the literature (Kim et al., 2002; Ntziachristos et al., 2007; Vu et al., 2015). For example, Ntziachristos et al. (2007) have reported number mode diameters of around 30 nm during a 7-week campaign next to a major freeway at Los Angeles. Moreover, previous particle number source apportionment studies have resolved factors with a similar mode diameter for the road traffic emissions (Beddows et al., 2015; Sowlat et al., 2016; Vu et al., 2016). For example, both Vu et al. (2016) and Beddows et al. (2015) reported road traffic factors with a number mode diameter at around 30 nm in an urban area in London. Factor 3 also shows correlations with tracers of traffic-related emissions, including NO_x, CO, and especially BC. Moreover, this factor does not have any correlation with number of departures and arrivals in the airport, suggesting that its origin is completely independent of the airport activities. All this evidence supports the identification of this factor as road traffic of the local pathways such as A4 and A9 freeways. The association of BC with this factor (67% factor loading) is considerably higher than the aircraft factors (i.e., departures and arrivals), which is consistent with the findings of Keuken et al. (2015, 2012), in which the authors observed significantly higher BC levels due to the local road traffic emissions than Schiphol airport emissions. Unlike its relatively low contribution to PNC (i.e., 18.0%), the resolved absolute concentration of this factor (i.e., 6298 particles/cm^3) is comparable with other values reported by source apportionment studies conducted in areas heavily impacted by traffic such as Beijing and Los Angeles (Liu et al., 2014; Sowlat et al., 2016). The modest relative contribution of this factor to PNCs (18.0%) is because of the dominance of airport emissions in the region. The pollution rose plot of this factor also supports its traffic origin (Fig. 5(c)). As can be seen in the figure, the winds blowing from west, southwest, and northwest facilitate the transport of traffic-related particles from the major surrounding freeways (e.g., A4 and A9).

Factor 4 (Ground service equipment (GSE)/local road traffic): Factor 4 has a number and volume mode diameter around 60–80 nm, and contributes to 6.5% of the total PNCs (Fig. 3 and Table 2). The corresponding absolute contribution of this factor to total PNCs was 2064 particles/cm^3 (Fig. 4). Moreover, the contribution of this factor to volume concentrations is 17.6%. Particles with the mode diameter of around 60–90 nm have been associated with HDVs and passenger buses (Huang et al., 2013; Wehner et al., 2009), which is consistent with the type of the ground-based vehicles in the airport. Previous source apportionment studies also reported a diesel-driven vehicle factor with number mode diameters of around 60–70 nm (Krecl et al., 2017, 2015), in agreement with the dominance of diesel fuel used in the airport ground-based operations. This factor is highly correlated (factor loadings of around 30–35%) with the exhaust-related tracers (e.g., CO and NO_x) as well. More importantly, it is correlated (factor loadings of around 25–40%) with both number of departures and arrivals in the airport. Therefore, this factor comprises mainly the ground service equipment (GSE) in the airport, which includes passenger buses and HDVs to transport luggage, fuel, and supply as mentioned in the introduction section, all of which increase with increasing flight numbers (both departures and arrivals). Moreover, we believe that this factor might include some minor contributions from local road traffic especially from the airport parking lots located to the northwest of the sampling site. Therefore, we labelled this factor as GSE/local road traffic. Moreover, based on the observed size mode and correlation with flight numbers and gaseous pollutants, this factor might also include contributions from auxiliary power units (APUs) as well (Ubogu et al., 2018), although some other studies suggest generally smaller mode diameters for APUs at different conditions (Khandelwal et al., 2019; Kinsey et al., 2012; Lobo et al., 2011). The pollution rose of this factor also corroborates its origin (Fig. 5(d)). The highest contributions are from southwest and northwest of the sampling site where the runways of the airport are located. Additionally, the contributions from northwest are comparable or even higher than those from southwest. This is likely because the runway located northwest of the sampling site is the farthest runway to the airport terminal. Therefore, the corresponding activities to transport passengers and luggage from the terminal to this runway emit more particles in the size range of this factor (i.e., 60–80 nm) from the northwest direction.

Factor 5 (Urban background): This factor is mostly characterized by particles larger than 100 nm, with the number and volume mode diameters of around 150–225 nm (Fig. 3). While this factor had a minimal contribution (a relative contribution of 2.7% and an absolute contribution of 936 particles/cm^3) to the total PNC (Fig. 4 and Table 2), it demonstrated the highest contribution in comparison to all of the other factors to the total volume concentrations (58.2%). Previous particle number source apportionment studies have indicated that such a number and volume mode at around 150–200 nm is typically associated with urban background particles, which have had the time to undergo atmospheric aging processes following their emission from a variety of pollution sources (e.g., industrial and residential sources, mixed road traffic, aviation, and shipping) of typical urban environments (Beddows et al., 2015, 2009; Masiol et al., 2017; Sowlat et al., 2016; Vu et al., 2016).

The evaluation of the auxiliary variables profile for this factor indicated very high loadings of $PM_{2.5}$ mass (i.e., 60%), quite consistent with the large contribution of this factor to PM volume/mass. In addition, high loadings (around 30–35%) of urban pollutants, such as NO_x and CO, were also observed for this factor. This is also in agreement with the results from previous studies, showing strong associations between this factor and urban pollution tracers (e.g., NO_x and CO) (Beddows et al., 2015, 2009; Masiol et al., 2017; Sowlat et al., 2016; Vu et al., 2016). Lastly, the pollution rose of this factor showed high contributions from all of the directions including the urban areas located to the northeast of the sampling site (Fig. 5(e)). All this evidence further substantiates the labeling of this factor as urban background particles.

4. Summary and conclusions

This study was the first of its type to identify and quantify the contribution of major airport activities (e.g., aircraft departures, aircraft arrivals, and GSE) to the PNCs observed in a sampling site adjacent to a populated area affected by the airport emissions. In addition to the selected time-resolved pollutant concentrations (e.g., CO, NO_x, BC, and $PM_{2.5}$), we used the number of arrivals and departures as a tool to distinguish airport activities and nearby roadway PNC sources. Our results showed that each of the airport activities and other nearby major combustion sources in the area are characterized by a distinct number size distribution. Despite the proximity of the sampling site to major airport runways, almost 20% of the PNC were explained by roadway traffic emissions from

nearby freeways, illustrating the need for multi-site source apportionment studies near PNC hotspots in urban areas. Based on the local wind patterns, the sampling site was intentionally selected to the northeast of Schiphol airport to capture the daily exposure of the populated areas located downwind of the airport. Aircraft departures had higher contributions to total PNC (46.1%) than arrivals (26.7%) in our sampling site, which is probably due to its proximity to the airport's busiest runways in terms of departure activities, longer departure taxing times and the departure/arrival activity schedule at the airport during the sampling hours of our campaign. As suggested by previous field studies, PNC levels due to aircraft activities might vary significantly depending on parameters such as the distance from the jet engine exhaust, engine type, fuel type, wind direction/frequency, and ambient conditions (e.g., temperature and relative humidity). Therefore, the findings of our study regarding PNC source contributions may only apply to the selected sampling area. Further research at different sites around airports with different geospatial characteristic (e.g., wind direction/speed, distance from major roadways and flight activity schedule) is needed to provide a finer resolution of source contributions of PNCs and their spatial variability in urban areas affected by airport activities.

CRediT authorship contribution statement

Milad Pirhadi: Conceptualization, Methodology, Software, Data curation, Writing - original draft. **Amirhosein Mousavi:** Methodology, Software, Data curation, Visualization. **Mohammad H. Sowlat:** Software, Data curation, Validation. **Nicole A.H. Janssen:** Investigation, Data curation, Resources. **Flemming R. Cassee:** Project administration, Supervision, Funding acquisition, Writing - review & editing. **Constantinos Sioutas:** Conceptualization, Project administration, Supervision, Writing - review & editing.

Acknowledgements

The authors wish to thank the USC Viterbi School of Engineering's PhD fellowship award for their support as well as John Boere, Paul Fokkens, Daan Leseman, Paul Schwillens and Jochem Klompmaker for the fieldwork. The field work of this study was funded by the Netherlands Ministry of Infrastructures and Water Management as part of grant M240045 and commissioned to the National Institute for Public Health and the Environment. The authors also wish to thank Dennis Mooibroek for the feedback on the methodology.

Appendix A. Supplementary data

Supplementary data to this article can be found online at https://doi.org/10.1016/j.envpol.2020.114027.

References

Beddows, D.C.S., Dall'Osto, M., Harrison, R.M., 2009. Cluster analysis of rural, urban, and curbside atmospheric particle size data. Environ. Sci. Technol. 43, 4694–4700.
Beddows, D.C.S., Harrison, R.M., Green, D.C., Fuller, G.W., 2015. Receptor modelling of both particle composition and size distribution from a background site in London, UK. Atmos. Chem. Phys. 15, 10107–10125.
Beyersdorf, A.J., Timko, M.T., Ziemba, L.D., Bulzan, D., Corporan, E., Herndon, S.C., Howard, R., Miake-Lye, R., Thornhill, K.L., Winstead, E., 2014. Reductions in aircraft particulate emissions due to the use of Fischer–Tropsch fuels. Atmos. Chem. Phys. 14, 11–23.
Brown, S.G., Eberly, S., Paatero, P., Norris, G.A., 2015. Methods for estimating uncertainty in PMF solutions: examples with ambient air and water quality data and guidance on reporting PMF results. Sci. Total Environ. 518, 626–635.
Chen, R., Hu, B., Liu, Y., Xu, J., Yang, G., Xu, D., Chen, C., 2016. Beyond PM2. 5: the role of ultrafine particles on adverse health effects of air pollution. Biochim. Biophys. Acta Gen. Subj. 1860, 2844–2855.
Cheng, H., Saffari, A., Sioutas, C., Forman, H.J., Morgan, T.E., Finch, C.E., 2016. Nanoscale particulate matter from urban traffic rapidly induces oxidative stress and inflammation in olfactory epithelium with concomitant effects on brain. Environ. Health Perspect. 124, 1537.
Delfino, R.J., Sioutas, C., Malik, S., 2005. Potential role of ultrafine particles in associations between airborne particle mass and cardiovascular health. Environ. Health Perspect. 113, 934–946.
Delhaye, D., Ouf, F.-X., Ferry, D., Ortega, I.K., Penanhoat, O., Peillon, S., Salm, F., Vancassel, X., Focsa, C., Irimiea, C., 2017. The MERMOSE project: characterization of particulate matter emissions of a commercial aircraft engine. J. Aerosol Sci. 105, 48–63.
Dodson, R.E., Houseman, E.A., Morin, B., Levy, J.I., 2009. An analysis of continuous black carbon concentrations in proximity to an airport and major roadways. Atmos. Environ. 43, 3764–3773.
Gietl, J.K., Lawrence, R., Thorpe, A.J., Harrison, R.M., 2010. Identification of brake wear particles and derivation of a quantitative tracer for brake dust at a major road. Atmos. Environ. 44, 141–146.
Harrison, R.M., Beddows, D.C.S., Dall'Osto, M., 2011. PMF analysis of wide-range particle size spectra collected on a major highway. Environ. Sci. Technol. 45, 5522–5528.
Harrison, R.M., Jones, A.M., Gietl, J., Yin, J., Green, D.C., 2012. Estimation of the contributions of brake dust, tire wear, and resuspension to nonexhaust traffic particles derived from atmospheric measurements. Environ. Sci. Technol. 46, 6523–6529.
He, R.-W., Shirmohammadi, F., Gerlofs-Nijland, M.E., Sioutas, C., Cassee, F.R., 2018. Pro-inflammatory responses to PM 0.25 from airport and urban traffic emissions. Sci. Total Environ. 640, 997–1003.
Herndon, S.C., Jayne, J.T., Lobo, P., Onasch, T.B., Fleming, G., Hagen, D.E., Whitefield, P.D., Miake-Lye, R.C., 2008. Commercial aircraft engine emissions characterization of in-use aircraft at Hartsfield-Jackson Atlanta International Airport. Environ. Sci. Technol. 42, 1877–1883.
Hopke, P.K., 2016. Review of receptor modeling methods for source apportionment Review of receptor modeling methods for source apportionment. J. Air Waste Manag. Assoc. 66, 237–259.
Hsu, H.-H., Adamkiewicz, G., Houseman, E.A., Spengler, J.D., Levy, J.I., 2014. Using mobile monitoring to characterize roadway and aircraft contributions to ultrafine particle concentrations near a mid-sized airport. Atmos. Environ. 89, 688–695.
Hu, S., Fruin, S., Kozawa, K., Mara, S., Winer, A.M., Paulson, S.E., 2009. Aircraft emission impacts in a neighborhood adjacent to a general aviation airport in Southern California. Environ. Sci. Technol. 43, 8039–8045.
Huang, C., Lou, D., Hu, Z., Feng, Q., Chen, Y., Chen, C., Tan, P., Yao, D., 2013. A PEMS study of the emissions of gaseous pollutants and ultrafine particles from gasoline-and diesel-fueled vehicles. Atmos. Environ. 77, 703–710.
Hudda, N., Fruin, S.A., 2016. International airport impacts to air quality: size and related properties of large increases in ultrafine particle number concentrations. Environ. Sci. Technol. 50, 3362–3370.
Hudda, N., Gould, T., Hartin, K., Larson, T.V., Fruin, S.A., 2014. Emissions from an international airport increase particle number concentrations 4-fold at 10 km downwind. Environ. Sci. Technol. 48, 6628–6635.
Keuken, M.P., Henzing, J.S., Zandveld, P., Van Den Elshout, S., Karl, M., 2012. Dispersion of particle numbers and elemental carbon from road traffic, a harbour and an airstrip in The Netherlands. Atmos. Environ. 54, 320–327.
Keuken, M.P., Moerman, M., Zandveld, P., Henzing, J.S., Hoek, G., 2015. Total and size-resolved particle number and black carbon concentrations in urban areas near Schiphol airport (The Netherlands). Atmos. Environ. 104, 132–142.
Keywood, M.D., Ayers, G.P., Gras, J.L., Gillett, R.W., Cohen, D.D., 1999. Relationships between size segregated mass concentration data and ultrafine particle number concentrations in urban areas. Atmos. Environ. 33, 2907–2913.
Khandelwal, B., Cronly, J., Ahmed, I.S., Wijesinghe, C.J., Lewis, C., 2019. The effect of alternative fuels on gaseous and particulate matter (PM) emission performance in an auxiliary power unit (APU). Aeronaut. J. 1–19.
Kim, S., Shen, S., Sioutas, C., Zhu, Y., Hinds, W.C., 2002. Size distribution and diurnal and seasonal trends of ultrafine particles in source and receptor sites of the Los Angeles basin. J. Air Waste Manag. Assoc. 52, 297–307.
Kinsey, J.S., 2009. Characterization of Emissions from Commercial Aircraft Engines during the Aircraft Particle Emissions eXperiment (APEX) 1 to 3. Office of Research and Development, US Environmental Protection Agency.
Kinsey, J.S., Dong, Y., Williams, D.C., Logan, R., 2010. Physical characterization of the fi ne particle emissions from commercial aircraft engines during the Aircraft Particle Emissions eXperiment (APEX) 1 e 3. Atmos. Environ. 44, 2147–2156.
Kinsey, J.S., Hays, M.D., Dong, Y., Williams, D.C., Logan, R., 2011. Chemical characterization of the fine particle emissions from commercial aircraft engines during the aircraft particle emissions experiment (APEX) 1 to 3. Environ. Sci. Technol. 45, 3415–3421.
Kinsey, J.S., Timko, M.T., Herndon, S.C., Wood, E.C., Yu, Z., Miake-Lye, R.C., Lobo, P., Whitefield, P., Hagen, D., Wey, C., 2012. Determination of the emissions from an aircraft auxiliary power unit (APU) during the Alternative Aviation Fuel Experiment (AAFEX). J. Air Waste Manag. Assoc. 62, 420–430.
Krecl, P., Hedberg Larsson, E., Ström, J., Johansson, C., 2008. Contribution of residential wood combustion and other sources to hourly winter aerosol in Northern Sweden determined by positive matrix factorization. Atmos. Chem. Phys. 8, 3639–3653.
Krecl, P., Johansson, C., Targino, A.C., Ström, J., Burman, L., 2017. Trends in black

carbon and size-resolved particle number concentrations and vehicle emission factors under real-world conditions. Atmos. Environ. 165, 155–168.
Krecl, P., Targino, A.C., Johansson, C., Ström, J., 2015. Characterisation and source apportionment of submicron particle number size distributions in a busy street canyon. Aerosol. Air Qual. Res. 15, 220–233.
Liu, Z.R., Hu, B., Liu, Q., Sun, Y., Wang, Y.S., 2014. Source apportionment of urban fine particle number concentration during summertime in Beijing. Atmos. Environ. 96, 359–369.
Lobo, P., Hagen, D.E., Whitefield, P.D., 2012. Measurement and analysis of aircraft engine PM emissions downwind of an active runway at the Oakland International Airport. Atmos. Environ. 61, 114–123.
Lobo, P., Whitefield, P.D., Hagen, D.E., Rye, L.J., Blakey, S., Wilson, C.W., Williams, P.I., Christie, S., Raper, D., Uryga-Bugajska, I., 2011. SAE E31 Methodology Development and Association PM Emissions Characteristics of Aircraft APUs Burning Conventional and Alternative Aviation Fuels.
Masiol, M., Harrison, R.M., 2014. Aircraft engine exhaust emissions and other airport-related contributions to ambient air pollution : a review Aircraft Particle Emissions eXperiment. Atmos. Environ. 95, 409–455.
Masiol, M., Harrison, R.M., Vu, T.V., Beddows, D., 2017. Sources of sub-micrometre particles near a major international airport. Atmos. Chem. Phys. 17.
Masiol, M., Vu, T.V., Beddows, D.C.S., Harrison, R.M., 2016. Source apportionment of wide range particle size spectra and black carbon collected at the airport of Venice (Italy). Atmos. Environ. 139, 56–74.
Mazaheri, M., Bostrom, T.E., Johnson, G.R., Morawska, L., 2013. Composition and morphology of particle emissions from in-use aircraft during takeoff and landing. Environ. Sci. Technol. 47, 5235–5242.
Mazaheri, M., Johnson, G.R., Morawska, L., 2011. An inventory of particle and gaseous emissions from large aircraft thrust engine operations at an airport. Atmos. Environ. 45, 3500–3507.
Mazaheri, M., Johnson, G.R., Morawska, L., 2008. Particle and gaseous emissions from commercial aircraft at each stage of the landing and takeoff cycle. Environ. Sci. Technol. 43, 441–446.
Norris, G., Duvall, R., Brown, S., Bai, S., 2014. Epa Positive Matrix Factorization (Pmf) 5.0 Fundamentals and User Guide Prepared for the Us Environmental Protection Agency Office of Research and Development, washington, Dc. Washington, DC.
Ntziachristos, L., Ning, Z., Geller, M.D., Sioutas, C., 2007. Particle concentration and characteristics near a major freeway with heavy-duty diesel traffic. Environ. Sci. Technol. 41, 2223–2230.
Onasch, T.B., Jayne, J.T., Herndon, S., Worsnop, D.R., Miake-Lye, R.C., Mortimer, I.P., Anderson, B.E., 2009. Chemical properties of aircraft engine particulate exhaust emissions. J. Propul. Power 25, 1121–1137.
Paatero, P., Eberly, S., Brown, S.G., Norris, G.A., 2014. Methods for estimating uncertainty in factor analytic solutions. Atmos. Meas. Tech. 7, 781–797.
Paatero, P., Tapper, U., 1994. Positive matrix factorization: a non-negative factor model with optimal utilization of error estimates of data values. Environmetrics 5, 111–126.
Pirhadi, M., Mousavi, A., Taghvaee, S., Shafer, M., Sioutas, C., 2019. Semi-volatile components of PM2.5 in an urban environment: Volatility profiles and associated oxidative potential. Atmos. Environ. https://doi.org/10.1016/j.atmosenv.2019.117197.
Ren, J., Liu, J., Li, F., Cao, X., Ren, S., Xu, B., Zhu, Y., 2016. A study of ambient fine particles at Tianjin International Airport, China. Sci. Total Environ. 556, 126–135.
Ruuskanen, J., Tuch, T., Ten Brink, H., Peters, A., Khlystov, A., Mirme, A., Kos, G.P.A., Brunekreef, B., Wichmann, H.E., Buzorius, G., 2001. Concentrations of ultrafine, fine and PM2. 5 particles in three European cities. Atmos. Environ. 35, 3729–3738.
Shirmohammadi, F., Lovett, C., Sowlat, M.H., Mousavi, A., Verma, V., Shafer, M.M., Schauer, J.J., Sioutas, C., 2018. Chemical composition and redox activity of PM0.25 near Los Angeles International Airport and comparisons to an urban traffic site. Sci. Total Environ. 610, 1336–1346.
Shirmohammadi, F., Sowlat, M.H., Hasheminassab, S., Saffari, A., Ban-weiss, G., Sioutas, C., 2017. Emission rates of particle number , mass and black carbon by the Los Angeles International Airport (LAX) and its impact on air quality in Los Angeles. Atmos. Environ. 151, 82–93.
Sowlat, M.H., Hasheminassab, S., Sioutas, C., 2016. Source apportionment of ambient particle number concentrations in central Los Angeles using positive matrix factorization (PMF). Atmos. Chem. Phys. 16, 4849–4866.
Stanier, C.O., Khlystov, A.Y., Pandis, S.N., 2004. Ambient aerosol size distributions and number concentrations measured during the Pittsburgh Air Quality Study (PAQS). Atmos. Environ. 38, 3275–3284.
Targino, A.C., Machado, B.L.F., Krecl, P., 2017. Concentrations and personal exposure to black carbon particles at airports and on commercial flights. Transport. Res. Transport Environ. 52, 128–138.
Ubogu, E.A., Cronly, J., Khandelwal, B., Roy, S., 2018. Determination of the effective density and fractal dimension of PM emissions from an aircraft auxiliary power unit. J. Environ. Sci. 74, 11–18.
Vu, T.V., Beddows, D.C.S., Delgado-Saborit, J.M., Harrison, R.M., 2016. Source apportionment of the lung dose of ambient submicrometre particulate matter. Aerosol. Air Qual. Res. 16, 1548–1557.
Vu, T.V., Delgado-saborit, J.M., Harrison, R.M., 2015. Review : particle number size distributions from seven major sources and implications for source apportionment studies. Atmos. Environ. 122, 114–132.
Wehner, B., Uhrner, U., Von Löwis, S., Zallinger, M., Wiedensohler, A., 2009. Aerosol number size distributions within the exhaust plume of a diesel and a gasoline passenger car under on-road conditions and determination of emission factors. Atmos. Environ. 43, 1235–1245.
Westerdahl, D., Fruin, S.A., Fine, P.L., Sioutas, C., 2008. The Los Angeles International Airport as a source of ultrafine particles and other pollutants to nearby communities. Atmos. Environ. 42, 3143–3155.
Wey, C.C., Anderson, B.A., Wey, C., Miake-Lye, R.C., Whitefield, P., Howard, R., 2007. Overview on the aircraft particle emissions experiment (APEX). J. Propul. Power 23, 898–905.
Wey, C.C., Anderson, B.E., Hudgins, C., Wey, C., Li-Jones, X., Winstead, E., Thornhill, L.K., Lobo, P., Hagen, D., Whitefield, P., 2006. Aircraft Particle Emissions Experiment (APEX).
Zhou, L., Kim, E., Hopke, P.K., Stanier, C.O., Pandis, S., 2004. Advanced factor analysis on Pittsburgh particle size-distribution data special issue of aerosol science and technology on findings from the Fine Particulate Matter Supersites Program. Aerosol Sci. Technol. 38, 118–132.
Zhu, Y., Fanning, E., Yu, R.C., Zhang, Q., Froines, J.R., 2011. Aircraft emissions and local air quality impacts from takeoff activities at a large International Airport. Atmos. Environ. 45, 6526–6533.